THE JOURNAL OF BIOLOGICAL CHEMISTRY
Vol. 278, No. 12, Issue of March 21, pp. 10112–10118, 2003

Printed in U.S.A.

Mapping Interactions between the Ca^{2+}-ATPase and Its Substrate ATP with Infrared Spectroscopy*

Received for publication, December 5, 2002, and in revised form, January 13, 2003
Published, JBC Papers in Press, January 21, 2003, DOI 10.1074/jbc.M212403200

Man Liu and Andreas Barth‡

From the Institut für Biophysik, Johann Wolfgang Goethe-Universität, Theodor-Stern-Kai 7, Haus 74, D-60590 Frankfurt am Main, Germany

Infrared spectroscopy has been used to map substrate-protein interactions: the conformational changes of the sarcoplasmic reticulum Ca^{2+}-ATPase upon nucleotide binding and ATPase phosphorylation were monitored using the substrate ATP and ATP analogues (2′-deoxy-ATP, 3′-deoxy-ATP, and inosine 5′-triphosphate), which were modified at specific functional groups of the substrate. Modifications to the 2′-OH, the 3′-OH, and the amino group of adenine reduce the extent of binding-induced conformational change of the ATPase, with particularly strong effects observed for the latter two. This demonstrates the structural sensitivity of the nucleotide-ATPase complex to individual interactions between nucleotide and ATPase. All groups studied are important for binding and interactions of a given ligand group with the ATPase depend on interactions of other ligand groups.

Phosphorylation of the ATPase was observed for ITP and 2′-deoxy-ATP, but not for 3′-deoxy-ATP. There is no direct link between the extent of conformational change upon nucleotide binding and the rate of phosphorylation showing that the full extent of the ATP-induced conformational change is not mandatory for phosphorylation. As observed for the nucleotide-ATPase complex, the conformation of the first phosphorylated ATPase intermediate $E1PCa_2$ also depends on the nucleotide, indicating that ATPase states have a less uniform conformation than previously anticipated.

Ligand binding to proteins controls vast numbers of cellular processes and has attracted great scientific and economic interest. Protein and ligand flexibility are important determinants of the interaction and often lead to ligand binding modes that are not anticipated from structures obtained with other ligands. To these "failure(s) of the rigid receptor hypothesis" (1) is added here an impressive example: induced-fit binding of nucleotides to the Ca^{2+}-ATPase. This finding stems from a systematic mapping of substrate-protein interactions with infrared (IR)[1] spectroscopy. New approaches like this are welcome in the field of ligand-protein recognition, since the most informative techniques, NMR and x-ray crystallography, are laborious and problematic for some systems. Methods like fluorescence and luminescence that require less expenditure also provide less molecular information. We expect that this technology gap will be bridged by IR spectroscopy.

IR spectroscopy, one of the methods of vibrational spectroscopy, provides direct information on the molecular level, is cost-effective, and can be universally applied from small soluble proteins to large membrane proteins under near-physiological conditions. Work summarized in recent reviews (2–5) has shown that the vibrational spectrum changes characteristically when a ligand binds to a protein. This provides a direct observation of ligand binding: no marker compound has to be introduced to report the binding process, as with many other methods. Previous work has mostly focused on individual interactions between a ligand and a protein by monitoring the influence of the protein environment on the vibrational frequency of a particular group of the ligand, the signal of which is identified in a complex vibrational spectrum with the help of isotopically labeled ligands (6–8).

Here we employ a different approach to probe the role of single functional groups of a ligand in the interaction with a protein: using IR spectroscopy we monitored the protein conformational change induced by binding of substrate analogues, which are modified at specific functional groups of the substrate. This identifies those functional groups that are important in the interaction with the protein; structure-interaction relationships are obtained that are similar to structure-activity relationships in drug development that relate the chemical structure of compounds to their pharmacological activity.

This work studies the ATP binding site of the sarcoplasmic reticulum (SR) Ca^{2+}-ATPase (9–12). The SR Ca^{2+}-ATPase, an intrinsic membrane protein of about 110-kDa molecular mass, catalyzes Ca^{2+} transport from the cytoplasm of muscle cells into SR for relaxing a flexed muscle. The energy required for this active transport process is provided by hydrolysis of the substrate ATP, which phosphorylates the ATPase at Asp^{351}. The specificity of the SR Ca^{2+}-ATPase for nucleotides is not high and not only ATP, but also some other nucleotides and non-nucleotide substrates enable Ca^{2+} uptake (13–18).

The ATPase structure (19) of the Ca^{2+}-loaded state $E1Ca_2$ shows three cytoplasmic domains, the nucleotide binding domain (N-domain), the phosphorylation domain (P-domain), and the actuator domain (A-domain). The structure has been solved with and without 2′,3′-*O*-(2,4,6-trinitrophenyl)adenosine 5′-monophosphate (TNP-AMP), which binds to the N-domain at

* This work was supported by Deutsche Forschungsgemeinschaft Grant Ba1887/2-1. The costs of publication of this article were defrayed in part by the payment of page charges. This article must therefore be hereby marked "*advertisement*" in accordance with 18 U.S.C. Section 1734 solely to indicate this fact.

‡ To whom correspondence should be addressed: Dept. of Biochemistry and Biophysics, Arrhenius Laboratories for Natural Sciences, Stockholm University, S-106 91 Stockholm, Sweden. Tel.: 46-8-16-2452; Fax: 46-8-15-5597; E-mail: Andreas.Barth@dbb.su.se.

[1] The abbreviations used are: IR, infrared; SR, sarcoplasmic reticulum; N-domain, the nucleotide binding domain; P-domain, the phosphorylation domain; A-domain, the actuator domain; TNP-AMP, 2′,3′-*O*-(2,4,6-trinitrophenyl)adenosine 5′-monophosphate; caged nucleotide, P^3-1-(2-nitrophenyl)ethyl nucleotides; A23187, calcium ionophore; AMPPNP, β,γ-imidoadenosine 5′-triphosphate; $E1Ca_2$, the nucleotide-free ATPase; $E1NTPCa_2$, the nucleotide-ATPase complex; DTGS, deuterated triglycine sulfate; MSA, maximum signal amplitude; IMPPNP, β,γ-iminoinosine 5′-triphosphate.

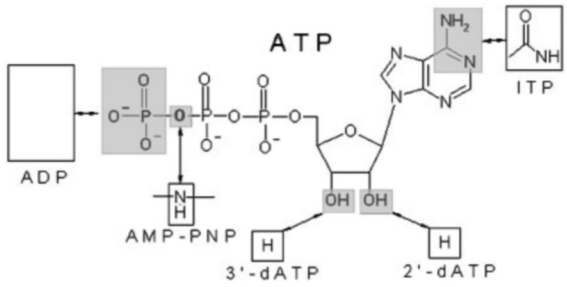

FIG. 1. **Structures of ATP and ATP analogues.**

considerable distance from the phosphorylation site Asp^{351} with less structural effects than ATP (20, 21). ATP is thought to bind to the surface of the N-domain with the phosphate groups pointing toward the phosphorylation site Asp^{351} (21), and most of the residues associated with the nucleotide binding site are located in the N-domain (12, 16, 20–24). Closure of the cleft between N- and P-domain is thought to occur to bring ATP close to Asp^{351} upon nucleotide binding (20, 21). In line with that, mutations at Asp^{351}, Lys^{352} (25), and Thr^{353} (26) alter the affinity of ATP to the ATPase.

IR spectroscopy has been used to characterize conformational changes of several partial reactions of the Ca^{2+}-ATPase pump cycle, as reviewed in Ref. 2. To detect the small IR absorbance changes generally associated with protein reactions, the reactions have to be triggered directly in the IR cuvette for which we use the photolytical release of nucleotides from photolabile derivatives, *i.e.* P^3-1-(2-nitrophenyl)ethyl nucleotides (caged nucleotides) (27). Here we characterize the conformational change induced by binding of the following ATP analogues: inosine 5′-triphosphate (ITP), 2′-deoxy-ATP, and 3′-deoxy-ATP (Fig. 1). They differ from ATP at individual functional groups which allows us to investigate the impact of these groups on the binding-induced conformational change.

EXPERIMENTAL PROCEDURES

Materials

IR samples were prepared as described previously (28). Approximate concentrations of the samples based on 1-μl sample volume were: 1.2 mM Ca^{2+}-ATPase, 0.5 mg/ml Ca^{2+} ionophore (A23187), 150 mM methylimidazole (pH 7.5), 150 mM KCl, 10 mM $CaCl_2$, 5 mM DTT, and 10 mM caged nucleotide. ITP samples were also prepared with 10 mM DTT because of a higher conversion of caged ITP in these samples.

In our control samples the nucleotide binding site was already saturated with β,γ-imidoadenosine 5′-triphosphate (AMPPNP) at the beginning of the experiment. The composition of these samples was the same as of that with caged AMPPNP (10 mM) except for the presence of AMPPNP (5 mM). Photolysis of caged AMPPNP in these samples did not lead to further nucleotide binding and conformational changes, they only revealed the effects of caged compound photolysis.

We did not use the physiological co-substrate Mg^{2+} but 10 mM Ca^{2+} instead. These conditions were chosen to block the $E1PCa_2 \rightarrow E2P$ transition to achieve a maximum level of $E1PCa_2$ in the steady state after nucleotide release while slowing down the phosphorylation reaction (29). Replacement of Mg^{2+} at the catalytic site by Ca^{2+} decreases the rate of phosphorylation by 1 order of magnitude (30–32), enabling a longer observation time for $E1ATPCa_2$ and therefore a better signal to noise ratio of the ATP binding spectrum. Ca^{2+} instead of Mg^{2+} has been used by us before (29, 33, 34) and gave very similar spectra for the $E1Ca_2 \rightarrow E1PCa_2$ (34) and the $E1Ca_2 \rightarrow E2P$ reaction (compare Fig. 6*A* of Ref. 34 and Fig. 4*a* of Ref. 29).

Methods

FTIR Measurements—Time-resolved Fourier transfer IR measurements of the Ca^{2+}-ATPase reaction were performed at 1 °C as described previously (28, 29). Photolytic release of nucleotides from their respective caged derivatives was triggered by a xenon flash tube or a XeCl excimer laser. Spectra were obtained in the following way: a reference spectrum was recorded with the protein in the $E1Ca_2$ state. After applying a photolysis flash or a sequence of flashes, we started to record time-resolved IR spectra with 65-ms time resolution. The number of photolysis flashes needed for saturating signals was determined as described under "Titration of IR Signals." Difference spectra were obtained by subtracting the reference spectrum from a spectrum obtained after nucleotide release. They reflect ATP binding and ATPase phosphorylation as well as the photolysis reaction. The spectra were normalized to a standard protein concentration before averaging spectra from different samples (amide II absorbance: 0.26) as described (35). A photolysis spectrum was then subtracted as described in the following paragraph to eliminate the photolysis band. The resulting spectra are named nucleotide binding spectra or $E1PCa_2$ formation spectra.

Subtraction of the Photolysis Spectrum—The spectrum obtained with the control samples shows only signals caused by the photolysis of caged AMPPNP. It is named *photolysis spectrum* and was used to subtract the photolysis bands from the raw difference spectra as described (33) using the same time interval for both spectra. This photolysis spectrum is identical to that of other caged nucleotides above 1300 cm^{-1}, *i.e.* outside the region of phosphate absorption.

Nucleotide Binding Spectra—For the nucleotide binding spectra time windows after the photolysis flash were evaluated in which the nucleotide-ATPase complex ($E1NTPCa_2$) accumulates. They were between 0.46 and 0.90 s for ATP or between 0.46 and 3.24 s for ATP analogues. 23 experiments from 12 samples were averaged for the ATP binding spectrum (~3 mM released ATP, one flash), four experiments from four samples for the ITP binding spectrum (~6.6 mM released ITP, three flashes), eight experiments from four samples for the 2′-deoxy-ATP binding spectrum (~3 mM released 2′-deoxy-ATP, one flash), and three experiments from three samples for the 3′-deoxy-ATP binding spectrum (~3 mM released 3′-deoxy-ATP, one flash).

Spectra of $E1PCa_2$ Formation—The difference spectra of $E1PCa_2$ formation ($E1Ca_2 \rightarrow E1PCa_2$) in Fig. 4 were obtained by subtracting the reference spectrum ($E1Ca_2$) from the spectrum of the protein in the $E1PCa_2$ state obtained in the time window between 4.5 and 28.1 s. A photolysis spectrum averaged in the same time window was subtracted using the same subtraction factors as for the respective nucleotide binding spectra.

Kinetics of Nucleotide Binding and Phosphorylation Reaction and Fitting Procedures—The time constants of nucleotide binding and ATPase phosphorylation were obtained by fitting the integrated band intensities of the marker band at 1628 cm^{-1} for nucleotide binding and two marker bands at 1721 and 1549 cm^{-1} for phosphorylation (29, 35) with the second (the third for ITP results) and first order exponential decay equations, respectively (Origin 5.0), and averaging the resulting time constants. 23 experiments were averaged for ATP, 8 for 2′-deoxy-ATP and 11 for ITP.

Titration of IR Signals—To obtain saturating signals, we titrated the amplitude of bands at 1641/1628 cm^{-1} by repeating an experiment on the same sample consisting of a reference spectrum, a photolysis flash, and a spectrum of 300 scans in a time interval when the first phosphoenzyme $E1PCa_2$ had formed. The number of flashes needed for saturating signals was used in further experiments.

Absorption Spectra of Nucleotides—Absorption spectra of 500 mM ATP, 2′- and 3′-deoxy-ATP dissolved in H_2O were measured using two BaF_2 windows (5-μm path length) with a Bruker Vector 22 spectrometer equipped with a deuterated triglycine sulfate (DTGS) detector at 20 °C at different pH values. The population of the $C_{2'}$-*endo* and $C_{3'}$-*endo* puckering modes of the three nucleotides were obtained by calculating the ratio of the areas of bands fitted to the spectrum near 830 cm^{-1} for $C_{2'}$-*endo* puckering and near 814 cm^{-1} for $C_{3'}$-*endo* puckering (36–38).

RESULTS

Titration of IR Signals with Nucleotide Binding—We first established the nucleotide concentration needed to obtain saturating IR signals. For that we used the difference in amplitude of the band pair at 1628 and 1641 cm^{-1} in the amide I region of the IR spectrum, which is sensitive to conformational changes. This difference is termed maximum signal amplitude (MSA). Fig. 2 shows the result of titrations with ATP, ITP, 2′-deoxy-ATP, and 3′-deoxy-ATP applying a total of eight flashes, which released ~9.4 mM nucleotide. According to Fig. 2, the binding-induced amplitude difference MSA reached saturating values with the first flash for ATP, 2′- and 3′-deoxy-ATP, and with the third flash for ITP. From the photolysis efficiency of 30% we then calculated the saturating nucleotide concentration

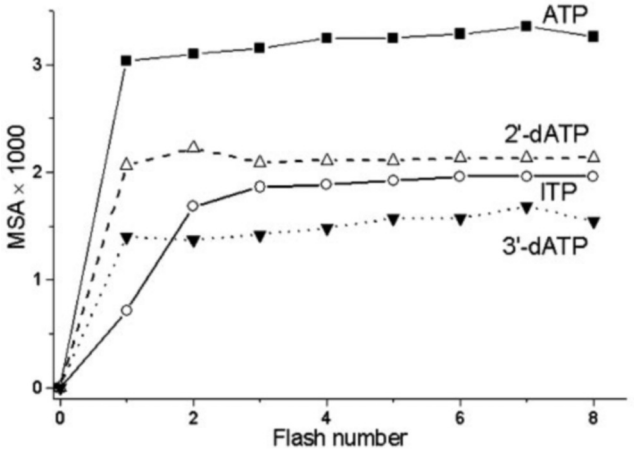

FIG. 2. **Titration of IR signals of E1PCa$_2$ formation (1 °C, pH 7.5).** MSA is the difference between the absorbance change at 1628 cm^{-1} and that at 1641 cm^{-1}. Data points are connected by lines to guide the eye of the reader. Approximate concentrations of the samples were: 1.2 mM Ca^{2+}-ATPase, 0.5 mg/ml Ca^{2+} ionophore (A23187), 150 mM methylimidazole, 150 mM KCl, 10 mM $CaCl_2$, 10 mM DTT, and 10 mM caged nucleotide.

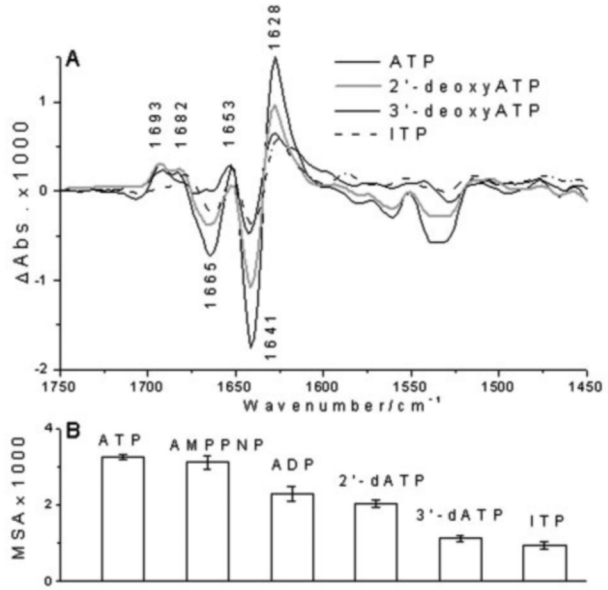

FIG. 3. *A*, nucleotide binding spectra (E1Ca$_2$ → E1NTPCa$_2$) of ATP, 2′-deoxy-ATP, 3′-deoxy-ATP, and ITP binding to the Ca^{2+}-ATPase (1 °C and pH 7.5). The labels indicate the band positions of the ATP binding spectrum. *B*, MSA values of the nucleotide binding spectra with S.D. *bars*. MSA is the difference between the absorbance change at 1628 cm^{-1} and that at 1641 cm^{-1} in the nucleotide binding spectra. In the samples there were: 1.2 mM Ca^{2+}-ATPase, 0.5 mg/ml Ca^{2+} ionophore (A23187), 150 mM methylimidazole, 150 mM KCl, 10 mM $CaCl_2$, 5 mM DTT (10 mM DTT for ITP samples), and 10 mM caged nucleotide.

assuming 1 μl of sample volume: 3 mM (one flash) for ATP and 2′- and 3′-deoxy-ATP and 6.6 mM (three flashes) for ITP.

For these titration experiments, spectra where evaluated in a time slot where the first phosphoenzyme E1PCa$_2$ accumulates. Strictly speaking, they have therefore determined the nucleotide concentration necessary for saturating E1PCa$_2$, not for saturating E1NTPCa$_2$. However, the reactions of nucleotide binding and of phosphorylation are well separated in time, which ensures that E1NTPCa$_2$ also saturates in the time slot evaluated for the nucleotide binding spectra: time constants for nucleotide binding (t_n) and phosphorylation (t_p) and the time slot of spectra recording for the nucleotide binding spectra (t_s) were: for ATP, $t_n \approx 0.11$ s, $t_p = 2.0$ s, $t_s = 0.46–0.90$ s; for 2′-deoxy-ATP, $t_n \approx 0.25$ s, $t_p = 6.7$ s, $t_s = 0.46–3.24$ s; for 3′-deoxy-ATP, $t_n \approx 0.49$ s, $t_p > 100$ s, $t_s = 0.46–3.24$ s; and for ITP, $t_n \approx 0.23$ s, $t_p = 8.66$ s, $t_s = 0.46–3.24$ s (see "Methods"). The starting time of 0.46 s for spectra averaging might seem to be early for ITP and 2′- and 3′-deoxy-ATP, since it is close to the time constant for nucleotide binding. However, increasing the starting time to 1.5 s for 3′-deoxy-ATP and 0.8 s for ITP and 2′-deoxy-ATP did not change the maximum signal amplitude MSA by more than 3%. Therefore we kept the time slot for averaging consistent for the three ATP analogues and as large as possible for an optimum signal to noise ratio.

Nucleotide Binding Spectra—Fig. 3*A* shows IR absorbance changes induced by nucleotide binding to the Ca^{2+}-ATPase. The spectra reflect the difference in absorbance between the initial nucleotide-free state E1Ca$_2$ and the nucleotide-ATPase complex E1NTPCa$_2$. Negative bands are characteristic of E1Ca$_2$ and positive bands of E1NTPCa$_2$. Groups or structures not involved in the conformational change do not show up in the difference spectra.

The difference spectra reflect conformational changes of the protein backbone in the amide I (1700–1610 cm^{-1}) and amide II (1580–1500 cm^{-1}) region of the spectra. In addition, environmental and structural changes of side chains and nucleotide contribute in the whole mid-IR region shown. We will focus here on the binding-induced absorbance changes in the amide I region.

The spectrum of ATP binding is in close agreement with the AMPPNP binding spectrum as noted before (33). The positive signal near 1653 cm^{-1} is characteristic of an α-helical structure, the signals near 1693, 1641, and 1628 cm^{-1} of β-sheets. Turn structures likely contribute to the signals near 1665 cm^{-1}. The spectrum indicates that α-helices, β-sheets, and turns are affected by ATP binding in line with previous findings (33).

The contour of all nucleotide binding spectra is similar; the main difference is the amplitude of the signals indicating various extents of conformational change. For further evaluation we used the MSA (difference between the absorbance change at 1628 cm^{-1} and that at 1641 cm^{-1}). As shown in Fig. 3*B*, the largest binding-induced signals were obtained with ATP and AMPPNP (28) (MSA $\approx 3 \times 10^{-3}$), medium size signals (MSA $\approx 2 \times 10^{-3}$) with ADP (28), and 2′-deoxy-ATP, and the smallest signals (MSA $\approx 1 \times 10^{-3}$) with ITP and 3′-deoxy-ATP. The different amplitudes of the nucleotide binding spectra cannot be explained by incomplete binding to the ATPase, since we have verified that saturating signals have been obtained (see above). MSA values shown in Fig. 3 for nucleotide binding spectra differ slightly from MSA values shown in Fig. 2, for which a time slot was evaluated in which E1PCa$_2$, not E1NTPCa$_2$, accumulated, because of conformational changes accompanying the phosphorylation reaction.

Spectra of Phosphoenzyme Formation—Phosphorylation leads to the appearance of two bands at 1721 and 1549 cm^{-1}, which serve here as marker bands for the first phosphorylated intermediate E1PCa$_2$ (29, 35). ATP, 2′-deoxy-ATP, and ITP, but not 3′-deoxy-ATP, phosphorylate the ATPase at a rate that is sufficiently high to observe accumulation of the E1PCa$_2$ state. Fig. 4 shows spectra of E1PCa$_2$ formation from E1Ca$_2$, *i.e.* the absorbance of E1PCa$_2$ minus the absorbance of E1Ca$_2$ (see "Methods"). As found for nucleotide binding, the shape of the E1PCa$_2$ formation spectra is similar for the analogues but the amplitude is different. In contrast, the *same* amplitude is observed for the band at 1721 cm^{-1}, which has been tentatively assigned to the C=O group of Asp^{351} formed upon phosphorylation (34, 35). This local probe of the phosphorylation reaction shows that E1PCa$_2$ accumulates to the same extent with ITP

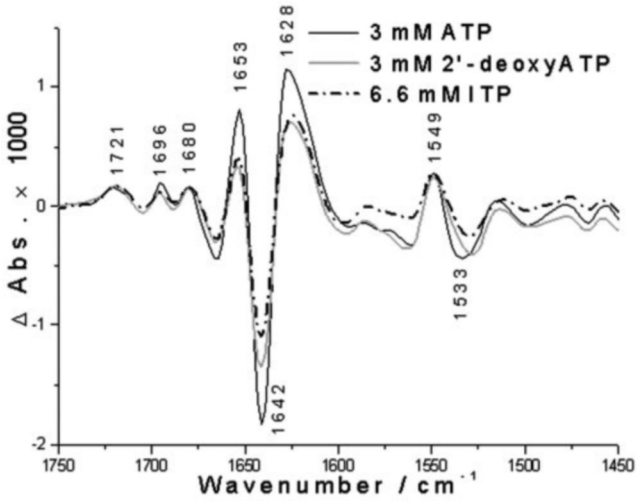

FIG. 4. **Spectra of $E1PCa_2$ formation ($E1Ca_2 \rightarrow E1PCa_2$) obtained with ATP, 2′-deoxy-ATP, and ITP.** Conditions are the same as described in the legend to Fig. 3.

and 2′-deoxy-ATP as with ATP. The smaller signals obtained with the analogues can therefore not be explained by incomplete phosphorylation. Instead they are due to a smaller extent of conformational change showing that the conformation of $E1PCa_2$ depends on the nucleotide used for phosphorylation of the ATPase.

Phosphorylation Rate—The rate of phosphorylation was measured using the marker bands at 1721 and 1549 cm^{-1} (29, 35). The kinetics of the two bands is shown in Fig. 5. Phosphorylation of the ATPase by 2′-deoxy-ATP or ITP is slower ($0.15 \pm 0.01\ s^{-1}$ and $0.12 \pm 0.01\ s^{-1}$, respectively) than by ATP ($0.51 \pm 0.03\ s^{-1}$). Slower phosphorylation of the ATPase with ITP and 2′-deoxy-ATP compared with ATP has been observed (39, 40), but without specifying the rate for ATP. Previous findings revealed a low phosphoenzyme concentration for both 2′- and 3′-deoxy-ATP (40), which we found only for 3′-deoxy-ATP. This is likely due to the different buffers used, since nucleotide binding (41) and the associated conformational change (28) depend on the composition of the medium.

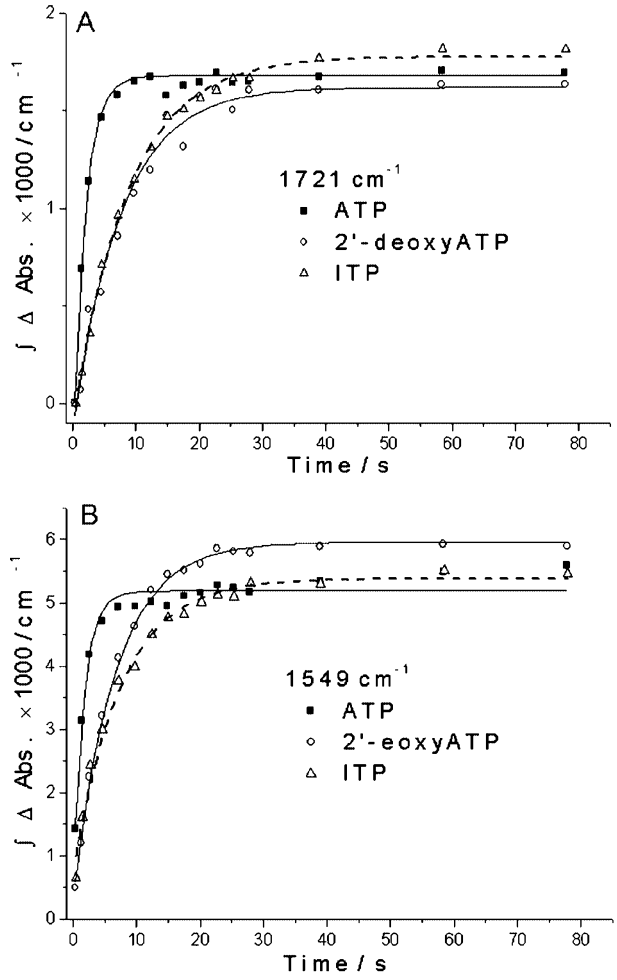

FIG. 5. **Kinetics of phosphoenzyme ($E1PCa_2$) formation with ATP, 2′-deoxy-ATP, and ITP at 1721 and 1549 cm^{-1}.** Conditions are the same as described in the legend to Fig. 3.

DISCUSSION

Interaction between ATPase and ATP—Our results show that modifications to the amino, 2′-OH, 3′-OH, and γ-phosphate groups of ATP affect the binding-induced conformational change of the ATPase. These groups are therefore important for the interaction between ATP and the ATPase. 3′-OH and the region near the amino group have the most significant influence on the induced-fit movement of the ATPase, since modification to either of these groups reduces the extent of backbone conformational change seen by IR spectroscopy to only one-third of that obtained with ATP. They are therefore important groups of ATP that anchor ATP to the ATPase. The importance of the functional groups of ATP investigated here for several partial steps of the ATPase reactions cycle has been shown before (39, 40, 42). The new finding here is that modifications of the ATP molecule have a direct effect on the structure of the nucleotide-ATPase complex. This is valid not only for side chain orientation as often found (1) but also for backbone conformation: with some ATP analogues the binding-induced conformational change of the backbone seen by the IR spectroscopy was found to be only one-third of that for ATP.

The effects of modifying ATP on nucleotide binding might have several causes: (i) a direct interaction of the modified group of ATP with the ATPase, (ii) a direct interaction of the "new" group of the ATP analogue, and (iii) an indirect effect on the interactions between protein and ATP via a change in electron density or conformation of ATP.

A direct interaction is the most likely cause for the reduced extent of conformational change observed for the deoxy-ATPs, since (i) no sterical restrains are expected from the replacement of the hydroxyl groups by the smaller hydrogen atoms, and (ii) effects on the equilibrium between sugar conformations of ATP in solution seem to be less relevant for the sugar conformation of the bound ATP molecule discussed as follows. 2′- or 3′-H substitution influence the sugar conformation in solution; according to the absorption spectra of ATP and 2′- and 3′-deoxy-ATP with deprotonated phosphate groups, the ratios of $C_{2'}$-*endo* and $C_{3'}$-*endo* puckering of these three nucleotides are 60:40, 80:20, and 70:30, respectively. This shows that free nucleotides prefer $C_{2'}$-*endo* puckering, particularly deoxynucleotides. Similar results for ATP and 2′-deoxy-ATP were obtained before (43–45). NMR investigations demonstrate that $C_{2'}$- and $C_{3'}$-*endo* types of conformations are in rapid equilibrium in solution (43), indicating only a small activation barrier between the conformations. Despite the predominant $C_{2'}$-*endo* puckering in solution, the ATPase seems to choose the $C_{3'}$-*endo* conformation for binding, as determined by NMR (45). Therefore the conformation of the nucleotide-ATPase complex will not depend on the predominant sugar puckering in solution and the effects of ribose OH substitution are best explained by direct interactions of the ribose hydroxyls with the ATPase.

It is less certain whether the reduced extent of conforma-

tional change found with ITP can be explained by a localized interaction between the amino group and the ATPase. In ITP the carbonyl group replaces the amino group of ATP, and one of the two endocyclic nitrogen atom is protonated. These alterations are not localized only on the amino group but will change the electron density distribution in the entire six-membered ring and its hydrogen bonding pattern. Therefore the interaction seems to be located on the six-membered ring of adenine. Since the most drastic alteration is at the amino group, it is likely, but not mandatory, that our results reflect a direct interaction of the ATPase with the amino group.

All functional groups of ATP investigated here are important for inducing the conformation of the ATP-ATPase complex that is competent for phosphoryl transfer. This is shown by the dependence of the phosphorylation rate on the modification of 2′-OH, 3′-OH, and the adenine amino group. Therefore, interactions distant from the phosphate groups contribute to approaching or forming the phosphate binding pocket. Binding of ATP to the ATPase turns out to be an interactive process where the formation of interactions of a given functional group of ATP is reinforced by interactions of other groups, which can be at the opposite end of the ATP molecule.

Distance between γ-Phosphate and Asp^{351}—Our data show that phosphorylation does not strictly depend on the full extent of the conformational change achieved by ATP binding. This is in line with the observation that pseudo substrates like acetyl phosphate are able to produce the same kind of phosphoenzyme as ATP (42), although they are not expected to induce the same conformational change as ATP, because their structures are even more different from ATP than those of the nucleotides investigated here.

There is no simple link between the extent of conformational change upon nucleotide binding and the ability to form the phosphoenzyme: (i) the extent is larger for 2′-deoxy-ATP than for ITP but the apparent phosphorylation rates are very close, and (ii) the extent is similar for ITP and 3′-deoxy-ATP, but significant phosphorylation is only observed for ITP. If the conformational change detected in our spectra and the distance between γ-phosphate and phosphorylation site Asp^{351} were correlated, a small conformational change would place the γ-phosphate further away from Asp^{351} than a larger one and result in slower phosphorylation. Therefore the conformational change seen in our spectra seems to be not or only weakly correlated with the distance between γ-phosphate and Asp^{351}. This finding is in line with models where the γ-phosphate in the nucleotide-ATPase complex is still some distance away from the phosphorylation site, as proposed by Hua *et al.* (46) for the Ca^{2+}-ATPase and Ettrich *et al.* (47) for the Na^+/K^+-ATPase. Then, the γ-phosphate arrives at the catalytic site only after nucleotide binding, which could take place during the conformational change after nucleotide binding that has been identified as the rate-limiting step for phosphorylation (48). A γ-phosphate in some distance to the phosphorylation site provides a possibility of binding a regulatory ATP molecule to the phosphoenzyme at the same site (49).

Concerted Conformational Change—The interactions between nucleotide and protein induce a concerted conformational change upon nucleotide binding: they join forces to induce strain in the protein. If one of the interacting groups is modified to become a less effective binder, the interactions with the respective binding pocket are impaired, the strain is relieved, and a smaller conformational change is produced. A weakened interaction therefore affects the conformational change as a whole instead of producing only local effects. This concept explains that the modifications of ATP studied reduce all bands in the amide I region of the difference spectrum. If an interaction between nucleotide and ATPase had only local effects on the protein structure, a weakened interaction would selectively reduce the amplitude of difference bands associated with that conformational change, but not of all of the bands as observed here. Particularly interesting is that functional groups of ATP, which interact with different domains of the protein, produce the same type of conformational change: the amino function is thought to interact with the N-domain (19, 24, 46) and the γ-phosphate with the P-domain (25, 26, 46). Despite that, the absence of the γ-phosphate in ADP (28) or of the adenine amino group in ITP both reduce the amplitude of the same bands. This shows that the concerted conformational change detected here is caused by interactions of the nucleotide with different protein domains: the N- and the P-domain.

Nucleotide-specific Conformation—Our results suggest that nucleotide binding induces a conformation that is characteristic of the bound nucleotide, as proposed earlier from experiments that did not monitor the conformation of the nucleotide-ATPase complex directly (50). In light of the known flexibility of the N-domain (51, 52), this conformation might represent an average conformation. The (average) conformation adopted in the ATPase-nucleotide complex seems to be very sensitive to individual interactions between ATPase and nucleotide, since the extent of conformational change depends dramatically on the presence of individual functional groups of ATP.

Our finding of a nucleotide specific conformation of the nucleotide-ATPase complexes is supported by previous reports, in which different effects of different nucleotides were found on fluorescence properties (17, 18, 53), partial reaction rates (54–57), protection against proteolysis (21), effects of aromatic compounds (58), nucleotide binding properties of mutants (25), and uncoupling (59).

The structures of the nucleotide-ATPase complexes studied differ in two aspects: (i) the extent of the conformational change induced by nucleotide binding differs as indicated by the different amplitudes of the amide I signals, and (ii) structural details of the nucleotide-ATPase complex differ as shown by the subtle differences of band positions and spectral shape among the nucleotide binding spectra.

A structure characteristic of the nucleotide is inferred not only for the nucleotide-ATPase complex but also for $E1PCa_2$ where the conformation of the phosphoenzyme depends on the nucleotide that was used for phosphorylation.

The small conformational change upon ITP binding observed here suggests that soaking $E1Ca_2$ crystals with β,γ-iminoinosine 5′-triphosphate (IMPPNP) may not disrupt the crystals as ATP does (19) because of the relatively small conformational change seen here for ITP. This may therefore enable the investigation of nucleotide binding at atomic resolution. The conformational change induced by ATP binding may then be extrapolated from the conformational change seen upon IMPPNP binding.

The Conformational Change Reflected in IR Spectra—Conformational changes in two regions of the protein were proposed to occur upon nucleotide binding (21): (i) movement of the N-domain toward the P-domain and (ii) movement of the A-domain toward the P-domain. The latter does not seem to contribute to a large extent to our spectra for the following reason: Danko *et al.* (21) studied protection of the ATPase against proteolytic attack by various nucleotides. This effect is thought to reflect a movement of the A-domain. They found no effect for ADP, indicating that ADP does not promote significant movement of the A-domain. Our IR spectra of nucleotide binding, however, show that ADP binding induces a conformational change, the extent of which is two-thirds of that induced by ATP (28) (Fig. 3*B*). This shows that the conformational change

of the A-domain contributes not or only to a small extent to the IR difference spectra.

Instead, it is likely that the anticipated hinge movement of the N- and P-domain upon ATP binding causes the amide I signals. The hinge movement will, however, not *directly* reflect in our spectra, because highly mobile structural elements give broad IR bands before and after the conformational change, which largely cancel in the difference spectrum. Therefore IR spectroscopy will largely miss a conformational change in the mobile hinge region *itself*. In line with this, only small bands in a limited spectral region (1660 to 1680 cm^{-1}) can be assigned to mobile structures, since they exchange their amide proton upon $^1H_2O/^2H_2O$ exchange (33). Instead the nucleotide binding bands in the amide I region are caused by backbone stretches within well defined and stable structures, since they are hardly affected by $^1H_2O/^2H_2O$ exchange (33). In line with this finding of conformational changes in well structured regions, NMR spectroscopy has detected changes of backbone conformation in the N-domain upon AMP binding (60).

These conformational changes in well structured regions might report the hinge movement indirectly, since a conformational change in the hinge region will also affect the connecting stretches. These stretches become more ordered the more they are incorporated into the domains and therefore give rise to distinct bands in the amide I region; a hinge movement will alter the relative orientation of the connecting amide groups and their hydrogen bonding and therefore affect their amide I signals. From these considerations we think that our spectra detect the hinge movement *indirectly* because it is reported by structured backbone stretches that link hinge and domains.

The Hinge Movement between N- and P-domain—The hinge movement upon nucleotide binding seems, however, to be less pronounced than anticipated in the structural models (61, 62). Fluorescence energy transfer experiments show that distances between fluorescence labels in the N- and the P-domain do not change between $E1Ca_2$ or an E2 conformation, as reviewed in Ref. 63. Of particular interest is the unchanged distance of two pairs of residues for which a change in distance is expected from the two x-ray structures (19, 46). The distance between Cys^{344} and Lys^{515} increases from 46 Å in E2 to 50 Å in $E1Ca_2$, and that between Cys344 and Glu439 changes from 38 Å in E2 to 45 Å in $E1Ca_2$. These distance changes should result in decreases in fluorescence energy transfer by 33 and 41%, respectively, which are not observed (64, 65).

The hinge movement can bring the N- and P-domain close together in the $E1Ca_2$ state, since they can be cross-linked with glutaraldehyde (66). The cross-linked cleft of $E1Ca_2$ resembles that of the E2 structure, since the cross-linked residues are only 5 Å apart in the E2 structure but 21 Å in the $E1Ca_2$ structure. In line with these experiments, closure of the hinge could be modeled with the N- and P-domain structures of $E1Ca_2$ without steric clashes, and this brings the two cross-linked residues as close as 4 Å (62). The mobility of the N-domain (51, 52) implies that it is likely to move rather independently from the rest of the protein and that the hinge angle might depend less on the E2 and $E1Ca_2$ state than expected from the crystal structures. The more closed conformation in E2 and the open cleft between the N- and P-domain in $E1Ca_2$ of the crystal structures therefore most likely do not represent the average conformation of these states in solution. They are probably adopted in the crystals because of crystal contacts that are made possible by the mobility of the N-domain in both states (51, 52). In solution the average position of the N-domain will be probably in between those observed in the two crystal structures. Therefore it is plausible to assume that the cleft is less open for $E1Ca_2$ in solution than in the $E1Ca_2$ crystal structure, and that upon nucleotide binding the hinge movement between the N- and P-domain will be smaller than anticipated from the crystal structure.

Our results demonstrate that IR spectroscopy can be used to map ligand-protein interactions and may become an important tool for research as well as for drug and herbicide optimization. In the particular case of ATP binding to the SR Ca^{2+}-ATPase, modifications to the 2′-OH, 3′-OH, and amino group of ATP reduce the induced-fit movement of the Ca^{2+}-ATPase, with the six-membered ring of adenine and the 3′-OH of ribose exerting key interactions. Nucleotide binding seems to be a flexible and interactive process: the conformation of the complex is characteristic of the bound nucleotide, and the interactions to a given ligand group depend on interactions of other ligand groups. This finding may also shed new light on the ongoing controversy on the number of nucleotide binding sites. Many of these studies have been conducted with ATP analogues. If binding of an ATP analogue induces a conformation that is characteristic of only that analogue, results with different analogues are not necessarily comparable and do not necessarily reflect the effects of ATP binding. Therefore we propose that some of the conflicting results can be explained by the different conformations of the complexes obtained with different analogues.

Acknowledgments—We thank W. Mäntele for continuous support, W. Hasselbach (Max-Planck-Institut, Heidelberg, Germany) for the gift of Ca^{2+}-ATPase and J. E. T. Corrie (National Institute for Medical Research, London) and F. von Germar for the preparation of caged compounds. We are grateful to C. Toyoshima for sharing unpublished results with us.

REFERENCES

1. Davis, A. M., and Teague, S. J. (1999) *Angew. Chem. Int. Ed.* **38,** 736–749
2. Barth, A., and Zscherp, C. (2000) *FEBS Lett.* **477,** 151–156
3. Wharton, C. W. (2000) *Nat. Prod. Rep.* **17,** 447–453
4. Carey, P. R., and Tonge, P. J. (1995) *Acc. Chem. Res.* **28,** 8–13
5. Deng, H., and Callender, R. (1999) *Methods Enzymol.* **308,** 176–201
6. Belasco, J. G., and Knowles, J. R. (1980) *Biochemistry* **19,** 472–477
7. Cepus, V., Scheidig, A. J., Goody, R. S., and Gerwert, K. (1998) *Biochemistry* **37,** 10263–10271
8. Baenziger, J. E., Miller, K. W., and Rothschild, K. J. (1993) *Biochemistry* **32,** 5448–5454
9. Hasselbach, W., and Makinose, M. (1961) *Biochem. Z.* **333,** 518–528
10. Hasselbach, W. (1974) in *The Enzymes* (Boyer, P. D., ed) 3rd Ed., pp. 431–467, Academic Press, New York
11. Andersen, J. P. (1989) *Biochim. Biophys. Acta* **988,** 47–72
12. Lee, A., and East, J. (2001) *Biochem. J.* **356,** 665–683
13. Hasselbach, W. (1979) *Top. Curr. Chem.* **78,** 1–56]
14. Hasselbach, W. (1981) in *Membrane Transport* (Bonting, S. L., and De Pont, J. J. H. H. M., eds) pp. 183–208, Elsevier Science Publishers B. V., Amsterdam
15. Inesi, G., and De Meis, L. (1985) in *The Enzymes of Biological Membranes* (Martonosi, A., ed) 2nd Ed., Vol. 3, pp. 157–191, Plenum Press, New York
16. McIntosh, D. B. (1998) *Adv. Mol. Cell Biol.* **23A,** 33–99
17. Lacapere, J.-J., Bennett, N., Dupont, Y., and Guillain, F. (1990) *J. Biol. Chem.* **265,** 348–353
18. Wakabayashi, S., and Shigekawa, M. (1990) *Biochemistry* **29,** 7309–7318
19. Toyoshima, C., Nakasako, M., Nomura, H., and Ogawa, H. (2000) *Nature* **405,** 647–655
20. MacLennan, D. H., and Green, N. M. (2000) *Nature* **405,** 633–634
21. Danko, S., Yamasaki, K., Daiho, T., Suzuki, H., and Toyoshima, C. (2001) *FEBS Lett.* **505,** 129–135
22. Andersen, J. P., and Vilsen, B. (1992) *Acta Physiol. Scand.* **146,** 151–159
23. Mcalennan, D. H., Clarke, D. M., Loo, T. W., and Skerjanc, I. S. (1992) *Acta Physiol. Scand.* **146,** 141–150
24. McIntosh, D. B., Woolley, D. G., Vilsen, B., and Andersen, J. P. (1996) *J. Biol. Chem.* **271,** 25778–25789
25. McIntosh, D.-B., Woolley, D.-G., MacLenna, D.-H., Vilsen, B., and Andersen, J.-P. (1999) *J. Biol. Chem.* **274,** 25227–25236
26. Clausen, J. D., McIntosh, D. B., Wooley, D. G., and Andersen, J. P. (2001) *J. Biol. Chem.* **276,** 35741–35750
27. Kaplan, J. H., Forbush, B., and Hoffman, J. F. (1978) *Biochemistry* **17,** 1929–1935
28. Liu, M., and Barth, A. (2002) *Biospectroscopy* **67,** 267–270
29. Barth, A., von Germar, F., Kreutz, W., and Mäntele, W. (1996) *J. Biol. Chem.* **271,** 30637–30646
30. Suzuki, H., Nakamura, S., and Kanazawa, T. (1994) *Biochemistry* **33,** 8240–8246
31. Shigekawa, M., Wakabayashi, S., and Nakamura, H. (1983) *J. Biol. Chem.* **258,** 8698–8707
32. Lacapere, J.-J., and Guillain, F. (1990) *J. Biol. Chem.* **265,** 8583–8589

33. Von Germar, F., Barth, A., and Mäntele, W. (2000) *Biophys. J.* **78,** 1531–1540
34. Barth, A., Kreutz, W., and Mäntele, W. (1994) *Biochim. Biophys. Acta* **1194,** 75–91
35. Barth, A., and Mäntele, W. (1998) *Biophys. J.* **75,** 538–544
36. Wartell, R. M., and Harrell, J. T. (1986) *Biochemistry* **25,** 2664–2671
37. Taillandier, E., Ridoux, J. P., Liquier, J., Leupin, W., Denny, W. A., Wang, Y., Thomas, G. A., and Peticolas, W. L. (1987) *Biochemistry* **26,** 3361–3368
38. Ouali, M., Letellier, R., Sun, J. S., Akhebat, A., Adnet, F., Liquier, J., and Taillandier, E. (1993) *J. Am. Chem. Soc.* **115,** 4264–4270
39. de Meis, L., and de Mello, M.-C.-F. (1973) *J. Biol. Chem.* **248,** 3691–3701
40. Coan, C., Amaral, J. A., and Verjovski-Almeida, S. (1993) *J. Biol. Chem.* **268,** 6917–6924
41. Hasselbach, W., and The, R. (1975) *Eur. J. Biochem.* **53,** 105–113
42. Bodley, A. L., and Jencks, W. P. (1987) *J. Biol. Chem.* **262,** 13997–14004
43. Schleich, T., Blackburn, B. J., Lapper, R. D., and Smith, I. C. P. (1972) *Biochemistry* **11,** 137–145
44. Davies, D. B., and Danyluk, S. S. (1974) *Biochemistry* **13,** 4417–4434
45. Clore, G. M., Gronenborn, A. M., Mitchinson, C., and Green, N. M. (1982) *Eur. J. Biochem.* **128,** 113–117
46. Hua, S., Inesi, G., Nomura, H., and Toyoshima, C. (2002) *Biochemistry* **41,** 11405–11410
47. Ettrich, R., Melichercik. M. Teisinger, J., Ettrichova, O., Krumscheid, R., Hofbauerova, K., Kvasnicka, P., Schoner, W., and Amler, E. (2001) *J. Mol. Model* **7,** 184–192
48. Petithory, J. R., and Jencks, W. P. (1986) *Biochemistry* **25,** 4493–4497
49. Bishop, J. E., Al-Shawi, M. K., and Inesi, G. (1987) *J. Biol. Chem.* **262,** 4658–4663
50. Rubtsov, A. M., Quinn, P. J., and Boldyrev, A. A. (1988) *FEBS Lett.* **238,** 240–244
51. Jona, I., Matko, J., and Martonosi, A. (1990) *Biochim. Biophys. Acta* **1028,** 183–199
52. Huang, S., and Squier, T. C. (1998) *Biochemistry* **37,** 18064–18073
53. Kubo, K., Suzuki, H., and Kanazawa, T. (1990) *Biochim. Biophys. Acta* **1040,** 251–259
54. Champeil, P., Riollet, S., Orlowski, S., Guillain, F., Seebregts, C. J., and McIntosh, D. B. (1988) *J. Biol. Chem.* **263,** 12288–12294
55. Hobbs, A. S., Albers, R. W., Froehlich, J. P., and Heller, P. F. (1985) *J. Biol. Chem.* **260,** 2035–2057
56. Ferreira, S. T., and Verjovski-Almeida, S. (1988) *J. Biol. Chem.* **263,** 9973–9980
57. Scofano, H. M., Vieyra, A., and De Meis, L. (1979) *J. Biol. Chem.* **254,** 10227–10231
58. Petretski, J. H., Wolosker, H., and De Meis, L. (1989) *J. Biol. Chem.* **264,** 20339–20343
59. Fortea, M. I., Soler, F., and Fernandez-Belda, F. (2000) *J. Biol. Chem.* **275,** 12521–12529
60. Abu-Abed, M., Mal, T.-K., Kainosho, M., Maclennan, D.-H., and Ikura, M. (2002) *Biochemistry* **41,** 1156–1164
61. Toyoshima, C., and Nomura, H. (2002) *Nature* **418,** 605–611
62. Xu, C., Rice, W. J., He, W., and Stokes, D. L. (2002) *J. Mol. Biol.* **316,** 201–211
63. Bigelow, D. J., and Inesi, G. (1992) *Biochim. Biophys. Acta* **1113,** 323–338
64. Stefanova, H. I., Mata, A. M., Gore, M. G., East, J. M., and Lee, A. G. (1993) *Biochemistry* **32,** 6095–6103
65. Mata, A. M., Stefanova, H. I., Gore, M. G., Khan, Y. M., East, J. M., and Lee, A. G. (1993) *Biochim. Biophys. Acta* **1147,** 6–12
66. McIntosh, D. B. (1992) *J. Biol. Chem.* **267,** 22328–22335